

Signal Enhancement of Hydroquinone and Catechol on Their Simultaneous Determination

A. J. Saleh Ahammad^{1,*}, M. A. Ullah¹, M. M. Hoque¹, M. A. Mamun¹, M. K. Alam¹, A. N. Anju¹,
M. N. Islam Mozumder¹, R. Karim¹, Subrata Sarker² and Dong Min Kim^{2,*}

¹ Department of Chemistry, Jagannath University, Dhaka 1100, Bangladesh

² Department of Materials Science and Engineering, Hongik University, Sejong 300116, South Korea

*E-mail: ajsahammad@chem.jnu.ac.bd, dmkim@hongik.ac.kr

Received: 1 February 2017 / Accepted: 11 June 2017 / Published: 12 July 2017

An activated glassy carbon electrode (GCE), prepared by applying a constant oxidation potential, can simultaneously determine hydroquinone (HQ) and catechol (CC). Here, we report on the modification of the electrochemical activation process of the GCE by applying a constant reduction potential preceded by the application of constant oxidation potential. The GCE activated through two-step electrochemical activation enhanced peak currents of HQ and CC compared to that activated only at a constant oxidation potential. The redox responses from the mixture of HQ and CC were easily resolved at the improved activated GCE. The peak potential separation of 110 mV was large enough for the simultaneous determination of HQ and CC. The oxidation peak currents of HQ and CC were linear over the range from 1 to 200 μ M with the detection limits (S/N= 3) of 37 and 26 nM, respectively.

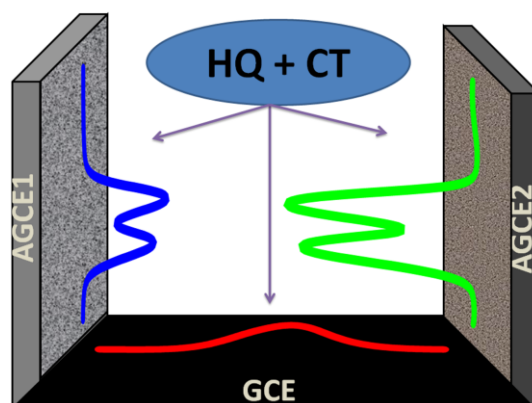
Keywords: Hydroquinone, Catechol, Activated glassy carbon electrode, Signal enhancement.

1. INTRODUCTION

Hydroquinone (HQ) and catechol (CC), isomers of dihydroxybenzene, are highly toxic; however, they are widely used in cosmetics, pesticides, photostabilizers, pharmaceuticals and other related industries [1]. US Environmental Protection Agency (EPA) and the European Union (EU) consider these two isomers of dihydroxybenzene as environmental pollutants since ingestion of certain amounts of these dihydroxybenzenes may pose threat to human health, animals, plants and aquatic life [2]. Owing to their similar structures and properties, they usually coexist in environmental samples and thus, it is not easy to separate them from their mixture [3]. Therefore, a simple and sensitive analytical method is highly desirable for simultaneous determination of HQ and CC.

Recently, electrochemical methods have attracted increasing attention because of their advantages of low cost, excellent selectivity, high sensitivity and simple operation [4, 5]. One big obstacle with the electrochemical method is that the voltammetric peaks corresponding to the oxidation of the isomers are largely overlapped at the conventional electrodes. In order to overcome this obstacle the electrodes are modified with conducting polymers [6], carbon nanotubes [7], gold nanoparticles [8], graphene [9], boron-doped diamond [10], etc. have been reported. However, the above modifications require sophisticated instruments, costly materials, and intricate methods. Glassy carbon electrode (GCE) is a widely used electrode material allows electrochemical measurements over a wide range of potentials. Electrochemically activated GCE (AGCE) can be considered as a modified electrode since an oxide layer is formed onto bare GCE after activation. Using AGCE is advantageous as the modification process is very simple and no extra modifiers are required. Previously, we reported AGCE, which was prepared by applying a constant oxidation potential, as a sensing platform to detect HQ and CC simultaneously [11].

In this study, we have shown that the peak currents of HQ and CC can be significantly enhanced with a simple variation of activation condition (Scheme 1). The enhancement of signals leads to improve the sensitivity and lower the detection limits of HQ and CC during their simultaneous determination.



Scheme 1. Graphical representation of the simultaneous detection of HQ and CC at GCE activated at a constant oxidation potential (AGCE1) and at a constant oxidation potential followed by a constant reduction potential (AGCE2).

2. EXPERIMENTAL

All reagents were obtained as analytical grade and used without further purification. Double distilled water was used to carry out all the experiments. Hydroquinone, catechol, sodium phosphate dibasic (Na_2HPO_4), sodium phosphate monobasic (NaH_2PO_4) and potassium ferricyanide were purchased from Sigma-Aldrich. 0.1 M pH 7.0 phosphate buffer solution (PBS) was used as the supporting electrolyte unless stated otherwise. The buffer solution was prepared following our previous procedure [11].

GCEs were polished with 0.05 μm alumina paste to a mirror-like surface. The polished GCEs were electrochemically activated in a 0.1 M PBS (pH 7.0) in two different ways as described elsewhere [11, 12]. In brief, the first activation was performed by applying a constant potential of +1.7 V for 400 s and named AGCE1. The second one, AGCE2, was obtained by two-step electrochemical activation, where a constant potential of +1.7 V for 400 s was followed by -1.0 V for 60 s. The activated GCEs were washed carefully with PBS and stored in a refrigerator (4 $^{\circ}\text{C}$) after use.

Voltammetric and impedimetric experiments were carried out with a CHI 660 E electrochemical workstation (CH Instruments, USA). A conventional three-electrode system was used where GCEs/ activated GCEs, an Ag/AgCl (3 M KCl) electrode, and a platinum wire were used as working, reference and counter electrodes, respectively.

3. RESULTS AND DISCUSSION

As mentioned above, AGCE1 and AGCE2 were obtained through the activation of GCE in two different ways. The electrochemical properties of activated GCEs differ from that of bare GCE due to the change of surface properties through activation. To investigate the electrochemical properties of AGCE1 and AGCE2, cyclic voltammograms (CVs) of $\text{K}_3[\text{Fe}(\text{CN})_6]$ were carried out as shown in Figure 1A.

Both the AGCE electrodes showed the characteristic reversible redox peaks. The peak currents were much lower with a less pronounced diffusional tail at AGCE1 due to the presence of negatively charged oxide layer at the AGCE1 that could restrict negatively charged $[\text{Fe}(\text{CN})_6]^{3-}$ from arriving at the electrode surface. On the other hand, the peak currents increased after reduction of the oxide layer (curve b), which suggested the AGCE2 had good conductivity and strong ability of electron transfer. This increase can be attributed to the cathodization step, which reduced the oxide layer and altered the nature of functional groups on the electrode surface [12]. Moreover, a possible mediation effect might be caused by the two-step electrochemical activation of electrode surface [13].

The different electron transfer properties of AGCE1 and AGCE2 were further investigated by electrochemical impedance spectroscopy (EIS) (Figure 1B) at a potential of 0.25 V that is, near the E° of $[\text{Fe}(\text{CN})_6]^{3-}$. The charge-transfer resistance (R_{ct}) for the $[\text{Fe}(\text{CN})_6]^{3-}$ redox couple at AGCE1 was larger than that at AGCE2. The results indicate that the electron transfer of negatively charged redox couple is hindered at the AGCE1 and vice versa for AGCE2, which is consistent with the results described in Figure 1A.

Figure 2 shows the DPV responses of HQ and CC at the GCE, AGCE1 and AGCE2. At the GCE, the oxidation peaks of HQ and CC appeared at 0.25 V and 0.30 V, respectively. The peak potentials shifted towards zero potential (0.07 V) at the activated GCEs. Moreover, the peak currents of HQ and CC increased at the activated GCEs. The peak currents significantly increased at AGCE2 for both HQ and CC. This is may be attributed to the increased surface conductivity of the AGCE2 through the application of a reduction potential.

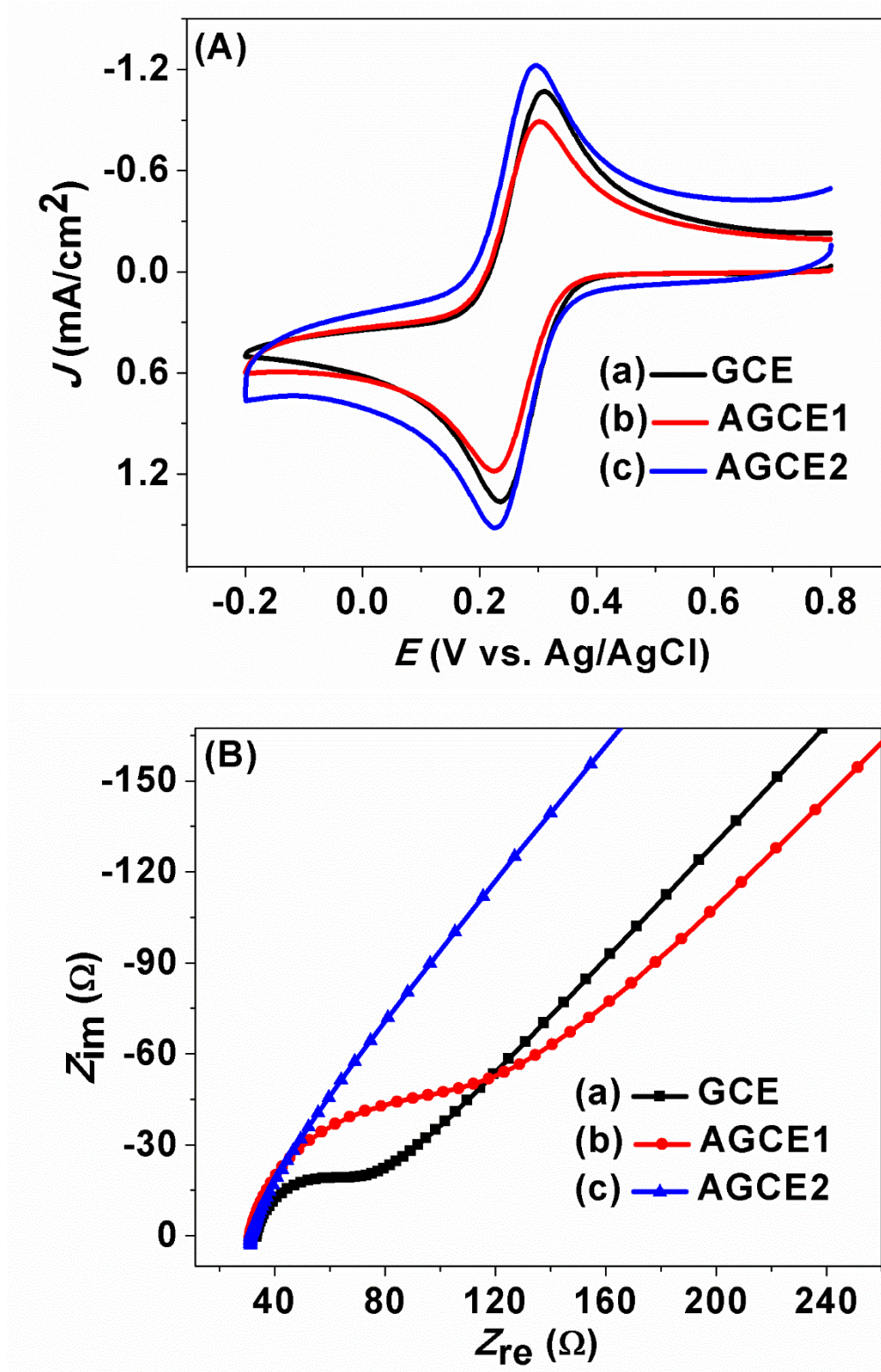


Figure 1. CVs (A) and EIS plots (B) of 5.0 mM $K_3[Fe(CN)_6]$ in 1 M KCl at GCE (a), AGCE1 (b), and AGCE2 (c).

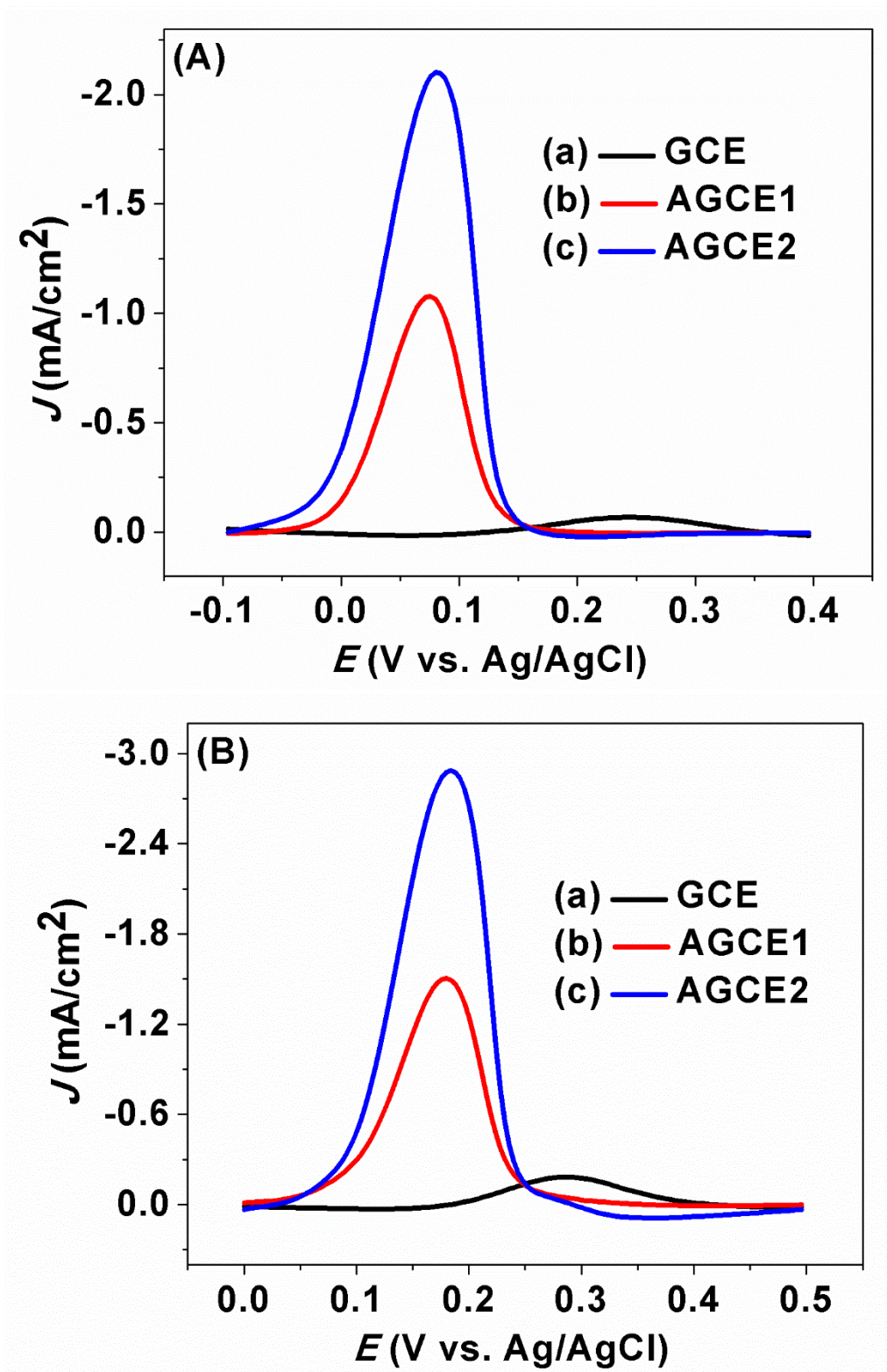


Figure 2. DPVs of 0.50 mM HQ (A) and CC (B) in PBS (pH = 7.0) at GCE (a), AGCE1 (b), and AGCE2 (c).

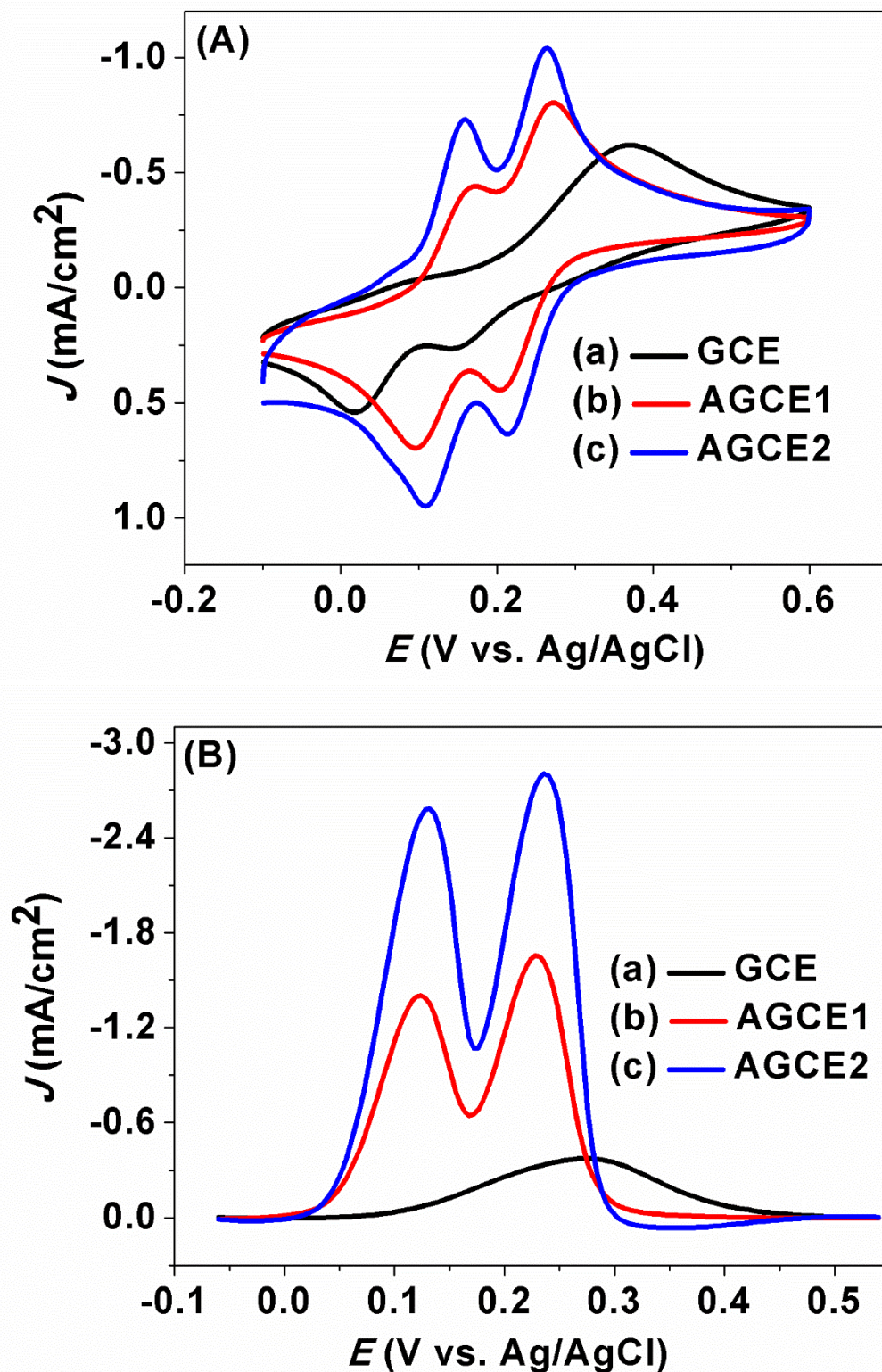


Figure 3. CVs (A) and DPVs (B) for the mixture solution of HQ (0.50 mM) and CC (0.50 mM) in PBS (pH = 7.0) at GCE (a), AGCE1 (b), and AGCE2 (c).

CVs and DPVs for the mixture of HQ and CC at the bare and activated GCEs were carried out as shown in Figure 3.

The oxidation waves of HQ and CC were clearly resolved in CV (Figure 3A) at the activated GCEs with peak potentials of 0.16 V and 0.26 V, respectively. On the other hand, the bare electrode showed an unresolved peak at 0.37 V. The electrochemical response of the mixture of HQ and CC was more pronounced in DPV (Figure 3B). Although HQ and CC were separated by 110 mV at both AGCE1 and AGCE2, the peak currents increased significantly at the AGCE2. Overall, we noted that AGCE2 showed much higher sensitivity on the resolution of these two components

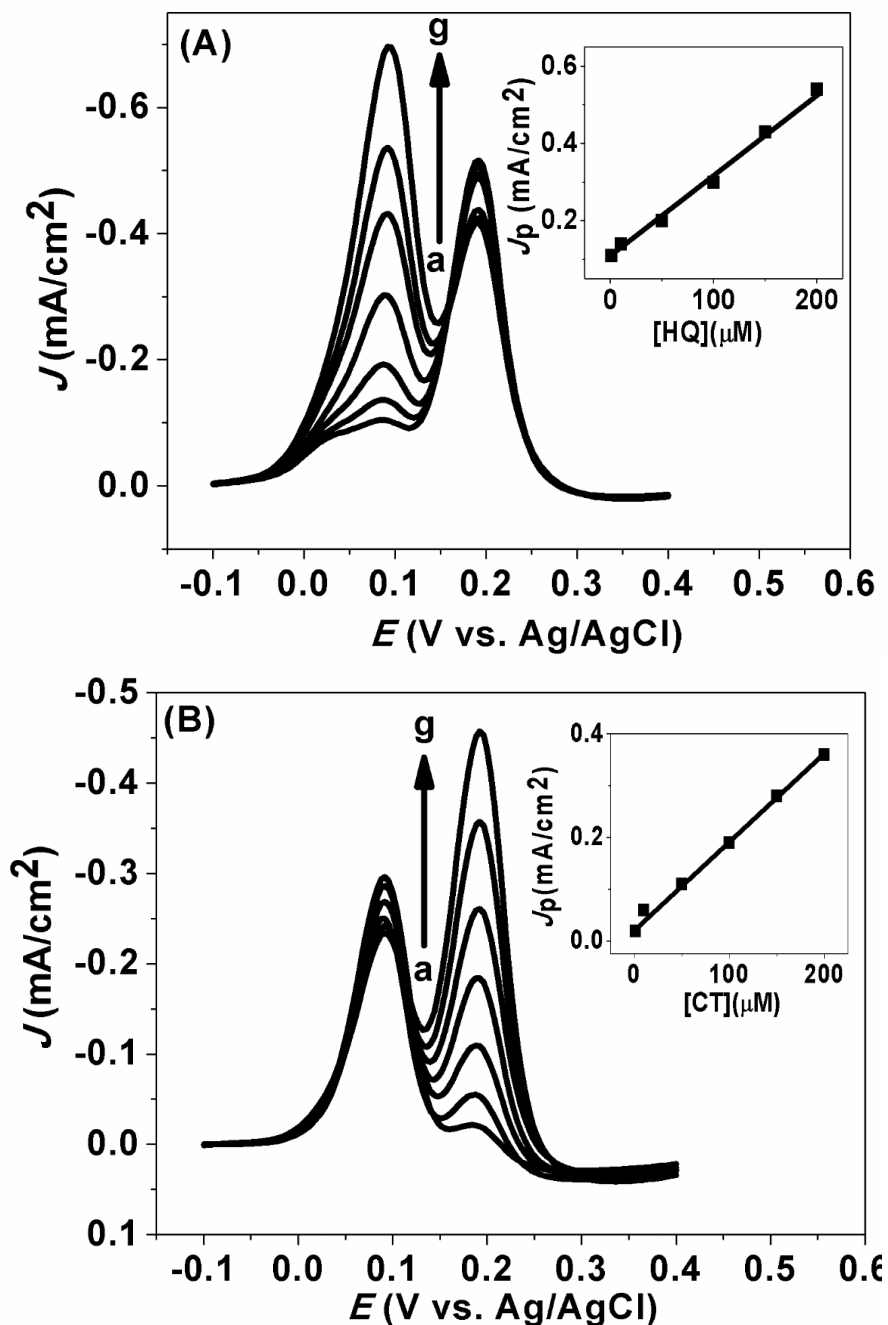


Figure 4. DPVs for AGCE2 in solution of different concentrations (a-g: 1, 10, 50, 100, 150, 200 and 300 μM) of HQ containing 150 μM CC (A) and different concentrations (a-g: 1, 10, 50, 100, 150, 200 and 300 μM) of CC containing 150 μM HQ (B). Insets show the calibration plots of HQ and CC.

Figure 4 shows the DPV responses at AGCE2 for the various concentrations of HQ and CC in the presence of a constant concentration of CC and HQ, respectively. The oxidation peak currents of HQ and CC increased linearly (up to 200 μM) as their concentration increased while the peak currents of the counterparts remained unchanged. The insets of Figure 4A and 4B show the calibration plots, which is constructed from the DPV responses for HQ and CC. The detection limits ($S/N=3$) for AGCE2 were estimated to be 37 nM and 26 nM for HQ and CC, respectively. These values were much lower than previously reported methods for the simultaneous detection of HQ and CC as shown in Table I.

Table 1. Comparison of the proposed method with others for the determination of HQ and CC.

Modified electrodes	Linear range, HQ; CC (μM)	Detection limits, HQ; CC (μM)	Reference
GCE/CNTs/CDs/CNTs/NF	1–200; 4–200	0.07, 0.06	[2]
AGCE1	0.5–200; 0.5–200	0.2 ; 0.1	[11]
GCE/RGO/GNPs	3–90; 3–300	0.15; 0.12	[14]
GCE/BDG	5–100; 1–75	0.3; 0.2	[15]
CMWNTs-LBL	10–120; 5–80	2.3; 1.0	[16]
GCE/CNTs-NTiO ₂	0.8–80; 0.8–80	0.09; 0.2	[17]
GR/CHI	0.2–110.6; 0.3–110.6	0.07; 0.09	[18]
GCE/MCMK-3	0.5–20; 0.5–25	0.1; 0.1	[19]
GCE/CNTs	1–100; 0.6–100	0.7 ; 0.2	[20]
GCE/NG	2.5–850, 1–650	0.5 ; 0.6	[21]
MEA/CNTs	1–100; 1–100	0.3 ; 0.2	[22]
GCE/PCA	15–115, 25–175	1.0 ; 0.6	[23]
GCE/APA	5–60, 1–60	0.9 ; 0.5	[24]
GCE/PGA	5–80; 1–80	1.0; 0.8	[25]
CPE/ECF	1–200; 1–200	0.4 ; 0.2	[26]
AGCE2	1–200; 1–200	0.04; 0.03	This work

NF: Nafion; CDs: carbon dots; CNTs : Carbon nanotubes; RGO: reduced graphene oxide; GNPs: gold nanoparticles; BDG: Boron-doped graphene; CMWNTs: carboxylated multi-wall carbon nanotubes; LBL: layer-by-layer; NTiO₂: nano-titanium dioxide; GR: graphite; CHI: chitin; MCMK-3: Mesoporous CMK-3; NG: Nano gold; MEA: Multielectrode array; PCA: Penicillamine; APA: Aspartic acid; PGA: Poly(glutamic acid); ECF: electrospun carbon nanofiber;

The relative standard deviation (RSD) for the oxidation peak currents of HQ and CC in 10 successive measurements were 0.53% and 0.72%, respectively, suggesting that the proposed method is

highly reproducible. After 40 consecutive CV measurements in the same condition, the peak currents of HQ and CC reduced to 97.9% and 98.2% of the initial responses, respectively. This revealed the good performance stability of the proposed sensor. In addition, the storage stability of the AGCE2 was also studied by keeping it in pH 7.0 PBS for three weeks at 4 °C. The peak current intensity decreased less than 5% of its initial response. Thus, it can be inferred that the proposed sensor possessed good storage stability to detect HQ and CC simultaneously and quantitatively.

4. CONCLUSIONS

In conclusion, we have shown that a simple variation of activation condition of GCE significantly increased the peak currents and lowered the detection limits of HQ and CC as well. This activation process is rather simple and no extra chemicals are required. The linear dynamic range was up to 200 μ M with the detection limit of 37 and 26 nM for HQ and CC, respectively. Further studies are still ongoing for full characterization and extension of this method to other activation condition and compare their sensitivity on the simultaneous detection of HQ and CC.

ACKNOWLEDGMENTS

This work was supported by the Ministry of Science and Technology of Bangladesh under the project 39.009.002.01.00.057.2015-2016/922/Phy's-24. SS and DMK acknowledge the support by the National Research Foundation of Korea (NRF) grant funded by the Ministry of Education, Science and Technology (MEST) of Korea under the project NRF-2011-00224237.

References

1. S. Hu, W. Zhang, J. Zheng, J. Shi, Z. Lin, L. Zhong, G. Cai, C. Wei, H. Zhang and A. Hao, *RSC Adv.*, 5 (2015) 18615.
2. C. Wei, Q. Huang, S. Hu, H. Zhang, W. Zhang, Z. Wang, M. Zhu, P. Dai and L. Huang, *Electrochim. Acta*, 149 (2014) 237.
3. Y. H. Huang, J. H. Chen, X. Sun, Z. B. Su, H. T. Xing, S. R. Hu, W. Weng, H. X. Guo, W. B. Wu and Y. S. He, *Sensor Actuat. B-Chem.*, 212 (2015) 165.
4. A. J. S. Ahammad, A. A. Mamun, T. Akter, M. A. Mamun, S. Faraezi and F. Z. Monira, *J. Solid State Electrochem.*, 20 (2016) 1933.
5. A. J. S. Ahammad, A. A. Shaikh, N. J. Jessy, T. Akter, A. A. Mamun and P. K. Bakshi, *J. Electrochem Soc.*, 162 (2015) B52.
6. A. J. S. Ahammad, M. M. Rahman, G. R. Xu, S. Kim and J. J. Lee, *Electrochim. Acta*, 56 (2011) 5266.
7. X. Wang, M. Wu, H. Li, Q. Wang, P. He and Y. Fang, *Sensor Actuat. B-Chem.*, 192 (2014) 452.
8. D. W. Li, Y. T. Li, W. Song and Y. T. Long, *Anal. Methods*, 2 (2010) 837.
9. H. J. Du, J. S. Ye, J. Q. Zhang, X. D. Huang and C. Z. Yu, *J. Electroanal. Chem.*, 650 (2011) 209.
10. J. Iniesta, P. Michaud, M. Panizza, G. Cerisola, A. Aldaz and C. Comninellis, *Electrochim. Acta*, 46 (2001) 3573.
11. A. J. S. Ahammad, S. Sarker, M. A. Rahman and J. J. Lee, *Electroanalysis*, 22 (2010) 694.
12. R. C. Engstrom and V. A. Strasser, *Anal. Chem.* 56 (1984) 136.

13. F. C. Moraesa, I. Cesarino, V. Cesarino, L. H. Mascaro, S. A.S. Machado, *Electrochim. Acta*, 85 (2012) 560.
14. S. Palanisamy, C. Karuppiyah, S. M. Chen, K. Muthupandi, R. Emmanuel, P. Prakash, M. S. Elshikh, M. A. Ali and F. M. A. A. Hemaïd, *Electroanalysis*, 27 (2015) 1144.
15. Y. Zhang, R. Sun, B. Luo and L. Wang, *Electrochim. Acta*, 156 (2015) 228.
16. S. Feng, Y. Zhang, Y. Zhong, Y. Li and S. Li, *J. Electroanal. Chem.*, 733 (2014) 1.
17. C. Wei, Y. Zhao, J. Huo, Q. Yang, C. Hu and Y. Zhang, *Int. J. Electrochem. Sci.*, 12 (2017) 1421.
18. S. Palanisamy, K. Thangavelu, S. M. Chen, V. Velusamy, T. W. Chen and R. S. Kannan, *J. Electroanal. Chem.*, 785 (2017) 40.
19. J. Yu, W. Du, F. Zhao and B. Zeng, *Electrochim. Acta*, 54 (2009) 984.
20. H. Qi and C. Zhang, *Electroanalysis*, 17 (2005) 832.
21. L. Han and X. Zhang, *Electroanalysis*, 21 (2009) 124.
22. D. Zhang, Y. Peng, H. Qi, Q. Gao and C. Zhang, *Sens. Actuator B-Chem.*, 136 (2009) 113.
23. L. Wang, P. F. Huang, J. Y. Bai, H. J. Wang, L. Y. Zhang and Y. Q. Zhao, *Microchim. Acta*, 158 (2007) 151.
24. L. Wang, P. F. Huang, H. J. Wang, J. Y. Bai, L. Y. Zhang and Y. Q. Zhao, *Ann. Chim.*, 97 (2007) 395.
25. L. Wang, P. Huang, J. Bai, H. Wang, L. Zhang and Y. Zhao, *Int. J. Electrochem. Sci.*, 2 (2007) 123.
26. Q. Guo, J. Huang, P. Chen, Y. Liu, H. Hou and T. You, *Sens. Actuator B-Chem.*, 163 (2012) 179.

© 2017 The Authors. Published by ESG (www.electrochemsci.org). This article is an open access article distributed under the terms and conditions of the Creative Commons Attribution license (<http://creativecommons.org/licenses/by/4.0/>).